CBGL: Fast Monte Carlo Passive Global Localisation for 2D LIDAR Sensors

Alexandros Filotheou

***Abstract*— Lorem ipsum dolor sit amet, consectetuer adipiscing elit. Ut purus elit, vestibulum ut, placerat ac, adipiscing vitae, felis. Curabitur dictum gravida mauris. Nam arcu libero, nonummy eget, consectetuer id, vulputate a, magna. Donec vehicula augue eu neque. Pellentesque habitant morbi tristique senectus et netus et malesuada fames ac turpis egestas. Mauris ut leo. Cras viverra metus rhoncus sem. Nulla et lectus vestibulum urna fringilla ultrices. Phasellus eu tellus sit amet tortor gravida placerat. Integer sapien est, iaculis in, pretium quis, viverra ac, nunc. Praesent eget sem vel leo ultrices bibendum. Aenean faucibus. Morbi dolor nulla, malesuada eu, pulvinar at, mollis ac, nulla. Curabitur auctor semper nulla. Donec varius orci eget risus. Duis nibh mi, congue eu, accumsan eleifend, sagittis quis, diam. Duis eget orci sit amet orci dignissim rutrum.**

CBGL leverages the relationships of (a) proportionality between the pose estimate error and the value of the Cumulative Absolute Error per Ray (CAER) metric for pose estimates in a neighbourhood of the origin, and (b) lack of disproportionality outside of that neighbourhood

***Index Terms*— global localisation, 2D LIDAR, monte carlo, scan–to–map-scan matching**

I. Introduction

This paper addresses the problem of Passive Global Localisation of a 2D LIDAR sensor, i.e. the estimation of its location and orientation within a given map, under complete locational and orientational uncertainty, without prescribing motion commands (to the mobile robot that the sensor is assumed mounted to) for further knowledge acquisition. Specifically the problem is formalised in Problem P:

Problem P. Let the unknown pose of an immobile 2D range sensor whose angular range is λ be $\boldsymbol{p}(\boldsymbol{l},\theta)$, $\boldsymbol{l} = (x,y)$, with respect to the reference frame of map $\boldsymbol{M}$. Let the range sensor measure range scan $\mathcal{S}_R$. The objective is the estimation of $\boldsymbol{p}$ given $\boldsymbol{M}$, λ, and $\mathcal{S}_R$.

II. Definitions

Let $\mathcal{A} = \{\alpha_i : \alpha_i \in \mathbb{R}\}$, $i \in \mathtt{I} = \langle 0,1,\ldots,n-1\rangle$, denote a set of n elements, $\langle\cdot\rangle$ denote an ordered set, $\mathcal{A}_\uparrow$ the set $\mathcal{A}$ ordered in ascending order, the bracket notation $\mathcal{A}[\mathtt{I}] = \mathcal{A}$ denote indexing, and notation $\mathcal{A}_{k:l}$, $0 \leq k \leq l$, denote limited indexing: $\mathcal{A}_{k:l} = \{\mathcal{A}[k], \mathcal{A}[k+1], \ldots, \mathcal{A}[l]\}$.

Definition I. *Range scan captured from a 2D LIDAR sensor.*—A conventional 2D LIDAR sensor provides a finite number of ranges, i.e. distances to objects within its range, on a horizontal cross-section of its environment, at regular angular and temporal intervals, over a defined angular range [1]. A range scan $\mathcal{S}$, consisting of N_s rays over an angular range λ, is an ordered map $\mathcal{S} : \Theta \to \mathbb{R}_{\geq 0}$, $\Theta = \{\theta_n \in [-\frac{\lambda}{2}, +\frac{\lambda}{2}) : \theta_n = -\frac{\lambda}{2} + \lambda\frac{n}{N_s}, n = 0,1,\ldots,N_s-1\}$. Angles

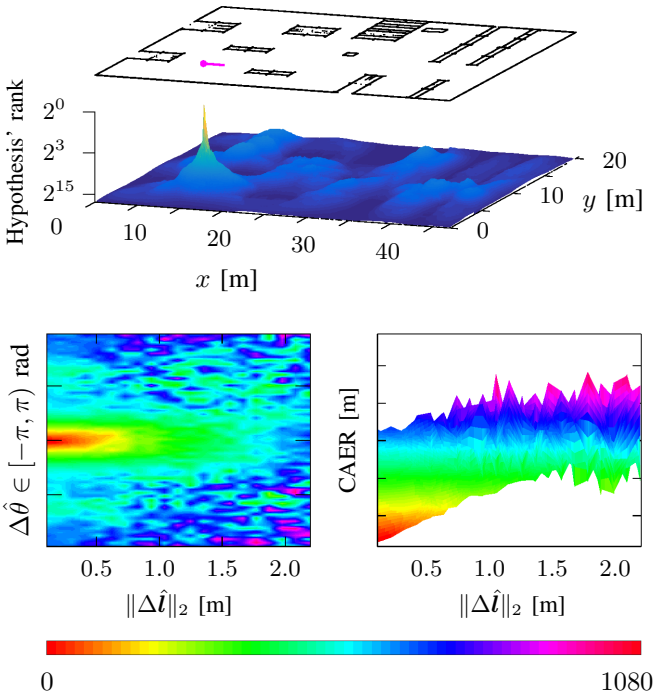

Fig. 1: Given a 2D LIDAR sensor's measurement, at its core, CBGL disperses pose hypotheses within the map and ranks them ascendingly according to the value of the CAER metric, producing a `r`(ank)-field which may be used to estimate the pose of the sensor (a) accurately due to the proportionality of estimate error and CAER, and (b) quickly due to the metric's low computational complexity. Top: a map of an environment, the pose of a panoramic 2D LIDAR sensor (magenta), and the corresponding CAER rank field below them. Bottom: distribution of CAER values by location and orientation error of all sensor pose hypotheses corresponding to the rank field above, for estimate distances up to 2.0 m. In this example the map's area is 800 m^2, and 10^6 hypotheses were dispersed randomly in its free space for 100 trials; CBGL's maximum location error and maximum execution time were, respectively, 0.062 m and 8.8 sec

θ_n are expressed relative to the sensor's heading, in the sensor's frame of reference.

Definition II. *Map-scan.*—A map-scan is a virtual scan that encapsulates the same pieces of information as a scan derived from a physical sensor. Only their underlying operating principle is different due to the fact the map-scan refers to distances to the boundaries of a point-set, referred to as the map, rather than within a real environment. A map-scan $\mathcal{S}_V^{\boldsymbol{M}}(\hat{\boldsymbol{p}})$ is derived by means of locating intersections of rays emanating from the estimate of the sensor's pose estimate $\hat{\boldsymbol{p}}$ and the boundaries of the map $\boldsymbol{M}$.

Definition III. *CAER as metric.*—Let $\mathcal{S}_p$ and $\mathcal{S}_q$ be two range scans, equal in angular range λ and size N_s. The value of the Cumulative Absolute Error per Ray (CAER) metric $\psi \in \mathbb{R}_{\geq 0}$ between $\mathcal{S}_p$ and $\mathcal{S}_q$ is given by

$$\psi(\mathcal{S}_p, \mathcal{S}_q) \triangleq \sum_{n=0}^{N_s-1} \left| \mathcal{S}_p[n] - \mathcal{S}_q[n] \right| \quad (1)$$

Definition IV. *CAER as field.*—A ψ-field on map $\boldsymbol{M}$ $f_\psi^{\boldsymbol{M}} : \mathbb{R}^2 \times [-\pi, +\pi) \to \mathbb{R}_{\geq 0}$ is a mappping of 3D pose configurations $\hat{\boldsymbol{p}}(\hat{x}, \hat{y}, \hat{\theta})$ to CAER values (def. III) such that if $\psi(\mathcal{S}_R, \mathcal{S}_V^{\boldsymbol{M}}(\hat{\boldsymbol{p}})) = c$ then $f_\psi^{\boldsymbol{M}}(\hat{\boldsymbol{p}}) = c$. In other words a CAER field is produced by computing the value of the CAER metric between a range scan $\mathcal{S}_R$ (def. I) and a map-scan $\mathcal{S}_V^{\boldsymbol{M}}(\hat{\boldsymbol{p}})$ captured from pose configuration $\hat{\boldsymbol{p}}$ within map $\boldsymbol{M}$ (def. II).

Definition V. *Rank field.*—Let $f_\psi^{\boldsymbol{M}}$ be a ψ-field on map $\boldsymbol{M}$ and $\mathcal{P} = \{\hat{\boldsymbol{p}}_i\}$, $i \in \mathtt{I} = \langle 0, 1, \ldots, |\mathcal{P}| - 1 \rangle$, be a set of 3D pose configurations within map $\boldsymbol{M}$, such that $f_\psi^{\boldsymbol{M}}(\mathcal{P}) = \Psi$. Let $\mathtt{I}^*$ be the set of indices such that $\Psi[\mathtt{I}^*] = \Psi_\uparrow$. A $\mathtt{r}$-field on map $\boldsymbol{M}$ $f_\mathtt{r}^{\boldsymbol{M}} : \mathbb{R}^2 \times [-\pi, +\pi) \to \mathbb{Z}_{\geq 0}$ is a mapping of 3D pose configurations $\mathcal{P}$ to non-negative integers such that if $f_\psi^{\boldsymbol{M}}(\mathcal{P}) = f_\psi^{\boldsymbol{M}}(\mathcal{P}[\mathtt{I}]) = \Psi$ then $f_\mathtt{r}^{\boldsymbol{M}}(\mathcal{P}[\mathtt{I}^*]) = \mathtt{I}$. In other words a rank field maps the elements of pose estimate set $\{\hat{\boldsymbol{p}}_i\}$ to the ranks $\mathtt{I}^*$ of their corresponding CAER values in hierarchy $\Psi_\uparrow$.

Definition VI. *Field densities.*—The locational and angular density, d_l and d_α respectively, of a ψ- or r-field express, correspondingly, the number of pose estimates per unit area of space and per angular unit.

III. Related Work

IV. The CBGL method

A. Motivation

The proposed method's motivation lies in the simple but powerful fact that, in general, is exhibited through figure 1: Assume a pose estimate residing in a neighbourhood of a 2D LIDAR sensor's pose within a given map; then the CAER metric between the scan measured by the sensor and the map-scan captured from the estimate within the map—the CAER metric is proportional to both the estimate's location error and orientation error. Formally the proposed method's foundations rest on Observation O:

Observation O. It may be observed that there are conditions such that Hypothesis H stands true.

Hypothesis H. There exists $\delta_0 \in \mathbb{R}_{>0}$ such that

- $\hat{\boldsymbol{p}} : \|\boldsymbol{p} - \hat{\boldsymbol{p}}\|_2 \leq \delta_0$ is an admissible pose estimate solution to Problem P, and
- set $\mathcal{V}$, as defined in Conjecture C, is non-empty

Conjecture C. Let the unknown pose of a 2D range sensor measuring range scan $\mathcal{S}_R$ (def. I) be $\boldsymbol{p}(x, y, \theta)$ with respect to the reference frame of map $\boldsymbol{M}$. Let $\mathcal{H}$ be a set of pose hypotheses within the free (i.e. traversable) space of $\boldsymbol{M}$: $\mathcal{H} = \{\hat{\boldsymbol{p}}_i(\hat{x}_i, \hat{y}_i, \hat{\theta}_i)\} \subseteq \mathtt{free}(\boldsymbol{M})$, $i \in \mathtt{I} = \langle 0, 1, \ldots, |\mathcal{H}| - 1 \rangle$. Let $f_\psi^{\boldsymbol{M}}$ be the ψ-field on $\boldsymbol{M}$ (def. IV) such that $f_\psi^{\boldsymbol{M}}(\mathcal{H}) = \Psi$. Let the field's locational and orientational densities be d_l and d_α. Let $\hat{\boldsymbol{p}}_\omega \in \mathcal{H}$ and $\psi_0, \delta_0 \in \mathbb{R}_{>0}$ such that $f_\psi^{\boldsymbol{M}}(\hat{\boldsymbol{p}}_\omega) = \psi_0$ and $\|\boldsymbol{p} - \hat{\boldsymbol{p}}_j\|_2 \leq \delta_0$ for all $\hat{\boldsymbol{p}}_j \in \mathcal{H} : f_\psi^{\boldsymbol{M}}(\hat{\boldsymbol{p}}_j) \leq \psi_0$. Let now $\mathcal{V} = \{\hat{\boldsymbol{p}}_i \in \mathcal{H} : f_\psi^{\boldsymbol{M}}(\hat{\boldsymbol{p}}_i) \leq \psi_0, \|\boldsymbol{p} - \hat{\boldsymbol{p}}_i\|_2 \leq \delta_0\}$. Without loss of generality there exist d_l, d_α, and ψ_0, δ_0 such that for all $\hat{\boldsymbol{p}}_\mathcal{V} \in \mathcal{V}$:

$$f_\psi^{\boldsymbol{M}}(\hat{\boldsymbol{p}}_\mathcal{V}) < f_\psi^{\boldsymbol{M}}(\hat{\boldsymbol{p}}) \quad \Leftrightarrow$$
$$\|\boldsymbol{p} - \hat{\boldsymbol{p}}_\mathcal{V}\|_2 < \|\boldsymbol{p} - \hat{\boldsymbol{p}}\|_2$$

for any $\hat{\boldsymbol{p}} \in \mathcal{X} = \mathcal{H} \setminus \mathcal{V} : \|\boldsymbol{p} - \hat{\boldsymbol{p}}\|_2 > \delta_0$.

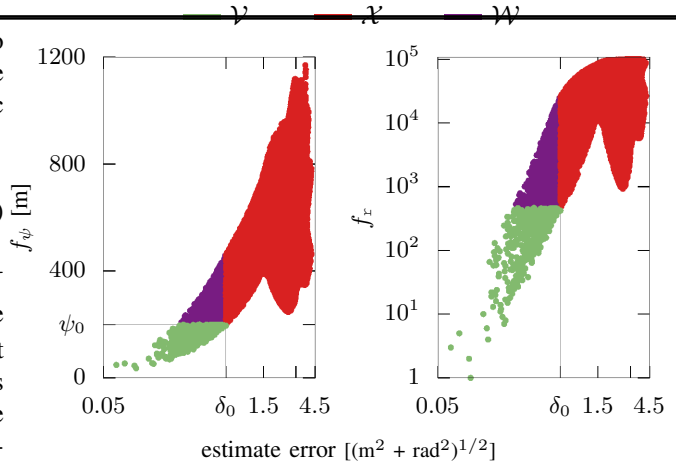

Fig. 2:

Remark I. The composition of $\mathcal{H} = \mathcal{V} \cup \mathcal{X} \cup \mathcal{W}$, where $\mathcal{W} = \hat{\boldsymbol{p}} \in \mathcal{H} \setminus \mathcal{V} : \|\boldsymbol{p} - \hat{\boldsymbol{p}}\|_2 \leq \delta_0$.

In simple terms Conjecture C states that, in general, given a dense enough set of pose hypotheses $\mathcal{H}$ over a map $\boldsymbol{M}$, it is possible to partition $\mathcal{H}$ into (non-empty) sets $\mathcal{V}$, $\mathcal{X}$, and $\mathcal{W}$ such that the error of pose estimates in set $\mathcal{V}$ and their corresponding CAER values are simultaneously lower than those of estimates in set $\mathcal{X}$.

B. The CBGL System

Lorem ipsum dolor sit amet, consectetuer adipiscing elit. Ut purus elit, vestibulum ut, placerat ac, adipiscing vitae, felis. Curabitur dictum gravida mauris. Nam arcu libero, nonummy eget, consectetuer id, vulputate a, magna. Donec vehicula augue eu neque. Pellentesque habitant morbi tristique senectus et netus et malesuada fames ac turpis egestas. Mauris ut leo. Cras viverra metus rhoncus sem. Nulla et lectus vestibulum urna fringilla ultrices. Phasellus eu tellus sit amet tortor gravida placerat. Integer sapien est, iaculis in, pretium quis, viverra ac, nunc. Praesent eget sem vel leo ultrices bibendum. Aenean faucibus. Morbi dolor nulla, malesuada eu, pulvinar at, mollis ac, nulla. Curabitur auctor semper nulla. Donec varius orci eget risus. Duis nibh mi, congue eu, accumsan eleifend, sagittis quis, diam. Duis eget orci sit amet orci dignissim rutrum.

Nam dui ligula, fringilla a, euismod sodales, sollicitudin vel, wisi. Morbi auctor lorem non justo. Nam lacus libero,

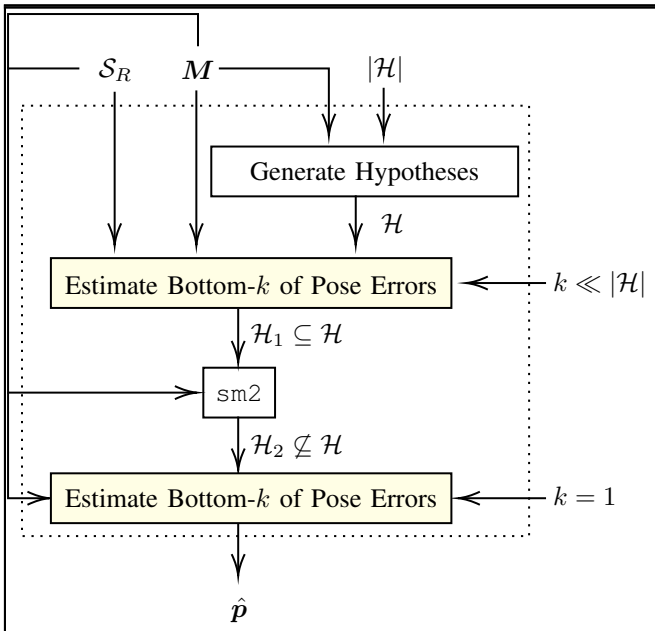

Fig. 3: CBGL in block diagram form. Given a LIDAR's 2D measurement $\mathcal{S}_R$ and the map $\boldsymbol{M}$ that represents the environment in which the sensor is posed, CBGL generates a set of pose hypotheses $\mathcal{H}$ and invokes the estimation of the k hypotheses with the least pose error (fig. 4; alg. II). Then it scan-to-map-scan matches those to the measurement for finer estimation and outlier rejection (alg. III). CBGL's output pose estimate is that with the least CAER among all similarly matched estimates

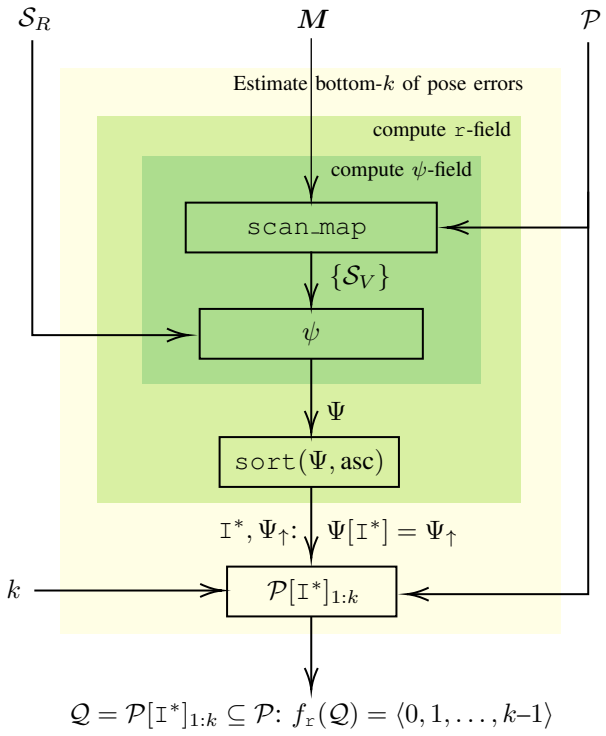

Fig. 4: CBGL's core method. Given a LIDAR's 2D measurement $\mathcal{S}_R$, the map $\boldsymbol{M}$ that represents the environment in which the sensor is posed, and a set of pose hypotheses $\mathcal{H}$, CBGL (a) computes and ranks the CAER values between the measurement and map-scans captured from the hypotheses within the map, and (b) outputs the hypotheses with the k lowest CAER values

Algorithm I: `CBGL`

Input: $\mathcal{S}_R$, $\boldsymbol{M}$, $|\mathcal{H}|$, k
Output: $\hat{\boldsymbol{p}}$

$\mathcal{H} \leftarrow \{\varnothing\}$
for $i \leftarrow 0, 1, \ldots, |\mathcal{H}| - 1$ **do**
  $\hat{\boldsymbol{p}}_i \leftarrow \mathtt{rand}(\hat{x}, \hat{y}, \hat{\theta}) : (x, y) \in \mathtt{free}(\boldsymbol{M})$
  $\mathcal{H} \leftarrow \{\mathcal{H}, \hat{\boldsymbol{p}}_i\}$
end for
$\mathcal{H}_1 \leftarrow \mathtt{bottom\_k\_poses}(\mathcal{S}_R, \boldsymbol{M}, \mathcal{H}, k)$ (Alg. II)
$\mathcal{H}_2 \leftarrow \{\varnothing\}$
for $k \leftarrow 0, 1, \ldots, |\mathcal{H}_1| - 1$ **do**
  $\hat{\boldsymbol{h}}' \leftarrow \mathtt{sm2}(\mathcal{S}_R, \boldsymbol{M}, \mathcal{H}_1[k])$ (Alg. III or e.g. `x1` [2])
  $\mathcal{H}_2 \leftarrow \{\mathcal{H}_2, \hat{\boldsymbol{h}}'\}$
end for
$\hat{\boldsymbol{p}} \leftarrow \mathtt{bottom\_k\_poses}(\mathcal{S}_R, \boldsymbol{M}, \mathcal{H}_2, 1)$
return $\hat{\boldsymbol{p}}$

Algorithm II: `bottom_k_poses`

Input: $\mathcal{S}_R$, $\boldsymbol{M}$, $\mathcal{H}$, k
Output: $\mathcal{H}_\triangledown$

$\Psi \leftarrow \{\varnothing\}$
for $h \leftarrow 0, 1, \ldots, |\mathcal{H}| - 1$ **do**
  $\mathcal{S}_V^h \leftarrow \mathtt{scan\_map}(\boldsymbol{M}, \mathcal{H}[h])$
  $\psi \leftarrow 0$
  for $n \leftarrow 0, 1, \ldots, |\mathcal{S}_R| - 1$ **do**
    $\psi \leftarrow \psi + \left|\mathcal{S}_R[n] - \mathcal{S}_V^h[n]\right|$ (Eq. (1))
  end for
  $\Psi \leftarrow \{\Psi, \psi\}$
end for
$[\Psi_\uparrow, \mathtt{I}^*] \leftarrow \mathtt{sort}(\Psi, \mathtt{asc})$
$\mathcal{H}_\triangledown \leftarrow \{\varnothing\}$
for $h \leftarrow 0, 1, \ldots, k - 1$ **do**
  $\mathcal{H}_\triangledown \leftarrow \{\mathcal{H}_\triangledown, \mathcal{H}[\mathtt{I}^*[h]]\}$
end for
return $\mathcal{H}_\triangledown$

Algorithm III: `sm2`

Input: $\mathcal{S}_R$, $\boldsymbol{M}$, $\hat{\boldsymbol{p}}$
Output: $\hat{\boldsymbol{p}}'$

$\mathcal{S}_V \leftarrow \mathtt{scan\_map}(\boldsymbol{M}, \hat{\boldsymbol{p}})$
$\boldsymbol{\Delta p} \leftarrow \mathtt{scan\text{-}match}(\mathcal{S}_R, \mathcal{S}_V)$ (e.g. `ICP` [3], `FSM` [4])
$\hat{\boldsymbol{p}}' \leftarrow \hat{\boldsymbol{p}} + \boldsymbol{\Delta p}$
return $\hat{\boldsymbol{p}}'$

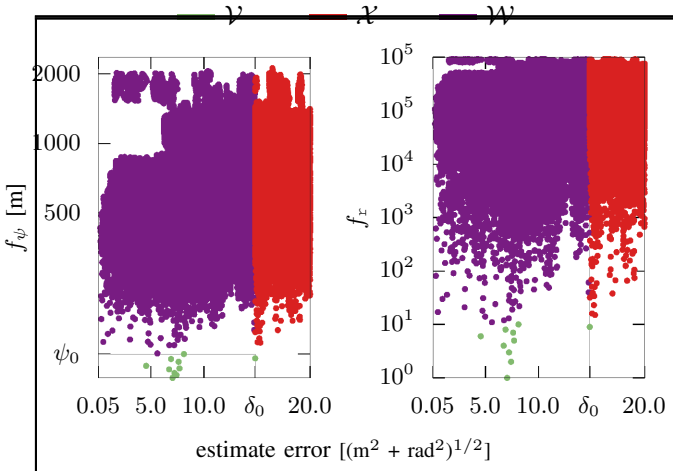

Fig. 5:

pretium at, lobortis vitae, ultricies et, tellus. Donec aliquet, tortor sed accumsan bibendum, erat ligula aliquet magna, vitae ornare odio metus a mi. Morbi ac orci et nisl hendrerit mollis. Suspendisse ut massa. Cras nec ante. Pellentesque a nulla. Cum sociis natoque penatibus et magnis dis parturient montes, nascetur ridiculus mus. Aliquam tincidunt urna. Nulla ullamcorper vestibulum turpis. Pellentesque cursus luctus mauris.

V. Experimental Evaluation

VI. Characterisation & Limitations

VII. Conclusion

References

[1] M. Cooper, J. Raquet, and R. Patton, "Range Information Characterization of the Hokuyo UST-20LX LIDAR Sensor," *Photonics*, 2018.

[2] A. Filotheou, A. L. Symeonidis, G. D. Sergiadis, and A. G. Dimitriou, "Correspondenceless scan-to-map-scan matching of 2D panoramic range scans," *Array*, 2023.

[3] I. Vizzo, T. Guadagnino, B. Mersch, L. Wiesmann, J. Behley, and C. Stachniss, "KISS-ICP: In Defense of Point-to-Point ICP Simple, Accurate, and Robust Registration If Done the Right Way," *IEEE Robotics and Automation Letters*, 2023.

[4] A. Filotheou, G. D. Sergiadis, and A. G. Dimitriou, "FSM: Correspondenceless scan-matching of panoramic 2D range scans," in *2022 IEEE/RSJ International Conference on Intelligent Robots and Systems (IROS)*. IEEE, 2022.